ELSEVIER

Journal of Crystal Growth 181 (1997) 351–362

JOURNAL OF CRYSTAL GROWTH

An atomic force microscopy study of super-dislocation/micropipe complexes on the 6H-SiC(0 0 0 1) growth surface

Jennifer Giocondi[a], Gregory S. Rohrer[a,*], Marek Skowronski[a], V. Balakrishna[b], G. Augustine[b], H.M. Hobgood[b], R.H. Hopkins[b]

[a] *Department of Materials Science and Engineering, Carnegie Mellon University, Pittsburgh, Pennsylvania 15213-3890, USA*
[b] *Northrop Grumman Science and Technology Center, 1310 Beulah Rd., Pittsburgh, Pennsylvania 15235, USA*

Received 16 August 1996; accepted 24 April 1997

Abstract

We have used atomic force microscopy (AFM) to study the (0 0 0 1) growth surface of a 6H-SiC single crystal at the points where micropipes emerge on the growth surface. All of the micropipes examined are origins of spiral steps, indicating that dislocations intersect the surface at these points. The dislocations observed at the surface/micropipe intersections have Burgers vectors of at least $4b_0$, where b_0 is the Burgers vector of a unit screw dislocation aligned along the c-axis ($b_0 = 15.19$ Å). Single and double unit dislocations were also observed, but they are not associated with micropipes. Micron-scale deposits of a heterogeneous phase were observed in the vicinity of the micropipes. The curvature of growth steps around these heterogeneities indicates that they impeded step motion while the crystal was growing. Based on our observations, we propose a model for the formation of super-dislocation/micropipe complexes that involves the coalescence of unit screw dislocations that are forced towards one another as large steps grow around heterogeneous material on the surface.

PACS: 61.72; 61.72.F

Keywords: Atomic force microscopy; SiC; Spiral growth; Screw dislocations; Micropipes

1. Introduction

Silicon carbide has properties that are superior to many currently used semiconductor materials. Its high thermal conductivity, breakdown field, saturation drift velocity, and bandgap make it particularly well-suited for high voltage power electronics [1]. The factor that has prevented wide-spread use of SiC for this application is the relatively high defect density in currently available wafers. Typical SiC wafers have dislocation densities in the 10^3–10^5 cm^{-2} range, voids, second phase

* Corresponding author. Fax: + 1 412 268 7596; e-mail: gr20@andrew.cmu.edu; www: http://neon.mems.cmu.edu/rohrer.html.

PII S0022-0248(97)00303-5

inclusions, and a type of defect characteristic of hexagonal semiconductors – micropipes [2–4]. Micropipes are empty tubes with diameters in the 1–10 μm range that can propagate along the *c*-axis, extend throughout most of the boule volume, and propagate into epilayers. Pipes are known to be detrimental to high voltage device operation; they cause premature breakdown through microplasma formation [5]. Typically, the density of micropipes is in the 50–10^3 cm^{-2} range and their density is usually higher in crystals with larger diameters [2, 4].

One plausible explanation for the stability of such a long, narrow cylindrical void was proposed by Frank in 1951 [6]. If a dislocation with a sufficiently large Burgers vector threads the length of a crystal, it can be energetically favorable to replace the most highly strained part of the crystal in the vicinity of the dislocation line with an empty cylinder. Frank demonstrated that a state of local equilibrium can be achieved by balancing the elastic energy of the dislocation against the surface energy of facets bounding a narrow cylinder. One of the central predictions of Frank's theory is that the pipe radius should be proportional to the square of the Burgers vector.

Several pieces of experimental evidence are available to support Frank's theory. First, Verma noted that micropipes intersect SiC growth surfaces at the origins of optically visible spiral steps [7]. Also, measurements based on optical micrographs of the growth surface have been used to show that the core radius increases with the height of the spiral step [8]. More recently, white beam synchrotron topography was used to show that micropipes in PVT grown 6H-SiC crystals were empty-core screw dislocations with Burgers vectors 3–7 times the *c* lattice constant [9]. A recent report by the current authors used atomic force microscopy (AFM) to make measurements that led to a similar conclusion; we found that all micropipes have Burgers vectors that are 4–13 times the *c* lattice constant [10]. In this same paper, it was also demonstrated that unit dislocations in 6H-SiC with a Burgers vector of only one *c* lattice constant do not form micropipes, and that for the super-dislocation/micropipe complexes, the micropipe radius increases with the square of the dislocation Burgers vector. Taken together, the results described above lead us to conclude that micropipes are empty-core super-dislocations as originally described by Frank [6]. Assuming that this explanation for the stability of the defect against closure or dissociation is essentially correct, then the next question to answer is, how do the super-dislocations (some with Burgers vectors as great as 200 Å) and their associated micropipes form in the growing crystal?

The objective of the present paper is to describe the structure of the 6H-SiC(0 0 0 1) growth surface in detail and, based on these observations, propose a model for the formation of micropipes. Topographic AFM images show that the crystal grows by the motion of large steps that emerge from spiral sources at surface/micropipe intersections. The distribution of the super-dislocation/micropipe complexes in the crystal indicates that screws of opposite sign are annihilated during the growth. We have also found that a heterogeneous phase is usually present near the surface/micropipe intersection. AFM images show that the heterogeneity impedes step motion and can nucleate voids in the space between dislocations. Based on these observations, a model is proposed for the formation of the super-dislocation/micropipe complexes.

2. Experimental procedure

All of the measurements described in this paper were conducted on the same 6H-SiC(0 0 0 1) growth surface. A wafer containing the growth surface was removed from the top of a large single crystal boule grown by the physical vapor transport (PVT) process [4]. In the PVT process, a powered SiC source at 2300–2400°C volatilizes and is transported to a somewhat cooler seed crystal held at 2100–2200°C. Under these conditions, the growth rates are in the range of 200–500 μm/h. The sample examined here was from a 1.5″ diameter 6H-SiC boule; no other polytypes were detected in this crystal. While this specimen was typical by most standards, it was selected for this study because it's micropipe density (approximately $10^3/cm^2$) exceeded that found in current state-of-the-art crystals. After sectioning, the crystal was imaged without further treatment using

a Park Scientific Instruments scanning probe microscope.

During our survey of the surface, an optical microscope was used to locate features of interest and to position the probe. Using the highest resolution scanner maximized the vertical sensitivity, but limited the field of view to 5 μm; larger areas of the surface had to be imaged by piecing together collages of smaller images. The relative positions of the individual images within each collage were determined on the basis of characteristic surface features; small misfits are due to nonlinearities in the scanner response that are amplified at the extreme edges of the field of view. Consistent images were recorded using a variety of probes and instrumental parameters. The contrast in each of the images that make up the collages was adjusted independently so that the relevant topographic features were visible. For example, in a part of the collage with no steps or a small step of unit height, the black-to-white contrast is on the order of 20 Å. Near one of the larger steps, it is a few hundred angstroms. This procedure allows features with a wide range of heights to be simultaneously visualized. The heights of important features are given in the description of each collage. Because a background plane is subtracted from each image, the whitest position of the image is typically found on the "uphill" side of the step and the blackest on the "downhill" side.

In the present analysis, we take the screw component of the dislocation's Burgers vector to be equal to the height of the step that emerges from the dislocation/surface intersection. This height can be determined directly from topographic AFM data, as illustrated in Fig. 1. Note that only the component of the Burgers vector normal to (0 0 0 1) is determined; topographic measurements can not be used to distinguish pure screw dislocations from those of mixed character. In order for rotating spiral steps to produce the 6H polytype, the step heights must occur in integer multiples of the c-axis repeat distance, which is the length of one unit screw dislocation along [0 0 0 1], $b_0 = 15.2$ Å. In fact, measured step heights seldom deviated from these intervals by more than a few angstroms (a few percent of the total height). In each case, therefore, step heights are assigned to the closest integer multiple of b_0. For example, the height of the step shown in Fig. 1 (136 Å) is very near $9b_0$.

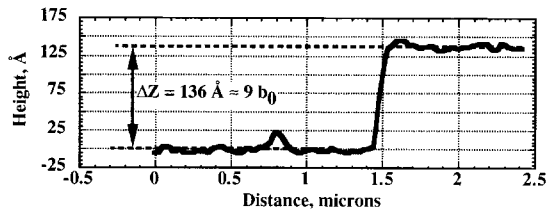

Fig. 1. Topographic AFM data. This is a single line scan over a step that emerges from a micropipe. It is assumed that all heights are integer multiples of the c-axis repeat distance.

3. Results

The growth surface of the SiC boule has a rounded dome shape. However, at the top of the crystal, in the center of the dome, there is a flat region made up of atomically smooth terraces, separated by large steps. Two characteristic areas of this flat region are shown for comparison in Fig. 2. Near the center, terraces are found which are separated by a combination of curved and straight steps, as illustrated in Fig. 2a. On the periphery of the flat region, the terraces are bounded by concentric rings. In Fig. 2b, small sections of these rings appear as lines that curve across the field of view. In both regions, the facets are decorated with smaller spiral steps that form 20–25 μm wide concentric terraces. Both clockwise and counter-clockwise spirals are observed but, instead of having a random distribution, spirals that rotate in the same direction are clustered in groups. For example, Fig. 3 shows a cluster of 5 spirals rotating in the counter-clockwise direction. The absence of screw dislocations with opposite Burgers vectors in the vicinity of the clusters indicates that some dislocation annihilation probably occurs as the crystal grows.

Note that in Fig. 3, there is a spot of black contrast at the origin of each spiral. This is where a micropipe emerges from the crystal. In many cases, such as the one shown in Fig. 4, multiple spirals emerge from a single micropipe. Fig. 4 is a collage of AFM images; the inset image is an optical micrograph of the same feature. In this and

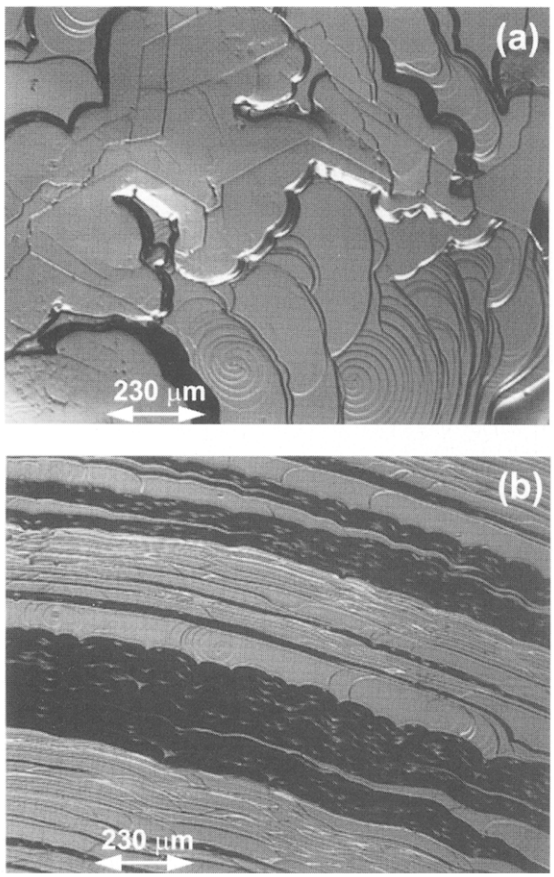

Fig. 2. Nomarski contrast optical micrographs of the 6H-SiC(0 0 0 1) growth surface in the flat central region on top of the boule. (a) Central region (b) Peripheral region.

all of the other AFM images presented here, dark contrast represents relatively low areas and lighter contrast represents relatively higher areas. Therefore, steps appear as continuous, abrupt changes in contrast and micropipes appear as black spots (at these voids, the probe extends to its lower limit). A Burgers circuit taken around this micropipe demonstrates that a dislocation with a screw component perpendicular to the surface must emerge from the crystal at this point. The steps labeled A_1 and A_2 are formed by a super-dislocation at the micropipe that has a magnitude of $13b_0$. The step labeled A_1 has a height of $7b_0$ and the step labeled A_2 has a height of $6b_0$. Note that in the region between the two large steps, where the contrast has been deliberately maximized to emphasize even the smallest heterogeneities, no other steps are observed.

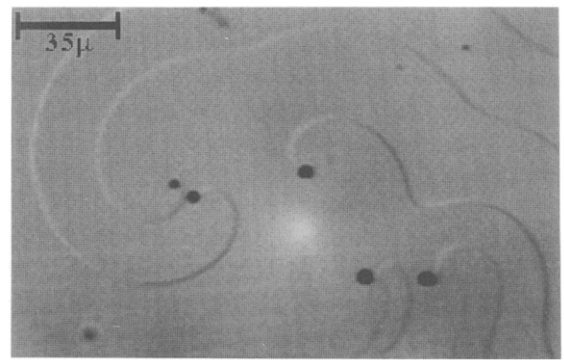

Fig. 3. Nomarski contrast optical micrograph showing a cluster of 5 super-dislocation/micropipe complexes. During growth, each spiral rotates in a counter-clockwise fashion. The annihilation of steps growing towards one another leads to the distorted shapes of the spirals.

While both of the steps in Fig. 4 were optically visible, in some cases single unit cell height steps emerge from the micropipe that are not observed in the optical microscope. For example, Fig. 5 shows a collage of AFM images that reveals one large 91 Å step (labeled A_1) and one smaller 15 Å step (labeled A_2) originating from a micropipe. While the larger of the two steps was visible in the optical microscope, the smaller one was not. Two other small steps (labeled A_3 and A_4), each 15 Å high, are found to terminate abruptly without a micropipe. The steps labeled A_1 and A_2 are the result of a super-dislocation which occurs at the micropipe and has a magnitude of $7b_0$. The steps labeled A_3 and A_4 are created by unit dislocations, each with a magnitude of b_0. This area is representative of our other observations.

During our survey of the surface, two micropipes were located in the optical microscope that did not have visible growth spirals. However, on closer examination with the AFM, we found that in both cases, multiple small steps, each with a height of b_0, emerged from the defect. Thus, based on our observations, we conclude that all micropipes are associated with super-dislocations that have Burgers vectors of Nb_0, where $N \geqslant 4$. Growth spirals

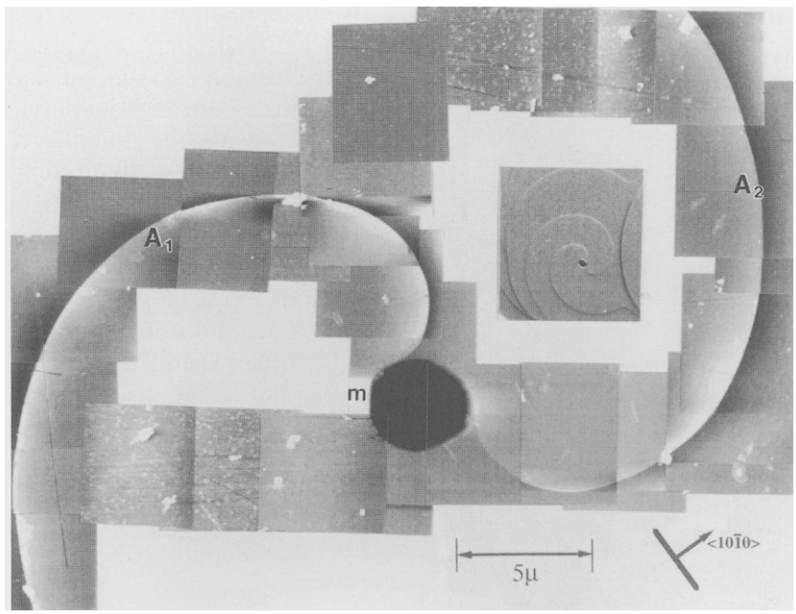

Fig. 4. A double spiral on the 6H-SiC(0 0 0 1) growth surface. The collage is formed from AFM images. The intersection of the micropipe with the surface is indicated with the "m". The inset is a Nomarski contrast optical micrograph of the same feature and is included to show the extended step structure of this defect.

formed by dislocations with small Burgers vectors where $N = 1$ or 2, on the other hand, terminate abruptly without forming a micropipe or depression. No dislocations with Burgers vectors of $3b_0$ were observed in this study.

The AFM images provide other important details about the characteristics of the surface/micropipe intersection. First, the dimensions and shape of the void are revealed. In an earlier report, we used this information to verify the parabolic relationship between the dislocation Burgers vector and the core radius [10]. Second, heterogeneous objects with micron-scale lateral dimensions appear to be scattered about on the growth surface and are often found in the vicinity of the micropipe. Isolated examples of such heterogeneities in Fig. 5 have white contrast (because they rise above the surface plane) and are labeled B_1 and B_2. While some fraction of these heterogeneities are mobile and can be moved by the scanning probe, those revealed in the images presented here are fixed to the surface and stable during repeated scanning. Although we cannot be certain that all of these objects were present on the surface during growth, some of them certainly were. For example, the heterogeneity labeled B_1 on Fig. 5 clearly influenced the progress of a growing step.

Interestingly, the heterogeneous material is most often found in the vicinity of the surface/micropipe intersection; one of the most instructive examples is shown in Fig. 6. As in Fig. 5, the heterogeneity has the lightest contrast because it rises 200–300 Å above the growth surface. Considering the fact that the steps curve around it (see positions indicated by the arrows), we can be certain that this heterogeneity was present during growth and that it is a phase other than SiC. The pattern in which the heterogeneity is distributed is characteristic of a liquid that has flowed, pooled, and solidified. Furthermore, the heterogeneity has well defined facets with angular separations (90° and 45°) that are characteristic of the low index planes of cubic crystals. If the inhomogeneous phase was liquid during growth, it was still able to prevent the steps

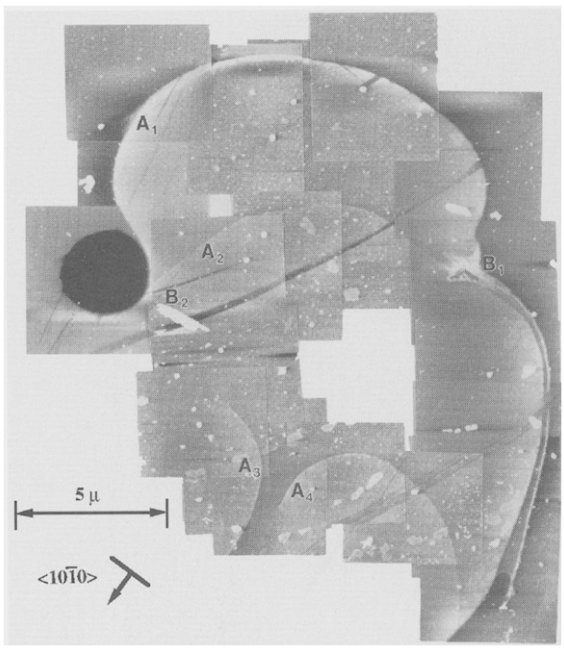

Fig. 5. A collage of AFM images showing a super-dislocation/micropipe complex and two unit dislocations, labeled A_3 and A_4. Note that the curvature of A_1 is altered where it is trying to grow around a region covered by heterogeneous material (the white contrast labeled B_1).

from advancing. While this particular micropipe shows more of the heterogeneous material than the others, similar heterogeneities are observed at the other defects. In most cases, the material is found on the slopes of the crater that is formed where the micropipe intersects the surface.

In addition to the micropipes with regular shapes shown in Figs. 4–6, we also observed a number of pipes with irregular shapes and one of them is shown in Fig. 7. Here, two spirals growing in the clockwise direction, each with is own oval-shaped void (labeled C_1 and C_2) are connected by a narrow channel (labeled D). A large heterogeneity (white contrast labeled B) lies in the channel and rises 200 Å above the surface of the surrounding crystal.

4. Discussion

All of the dislocations observed at micropipes have Burgers vectors at least 4 times b_0 and should, therefore, be unstable with respect to dissociation into an independent set of unit dislocations. Based on the fact that the super-dislocations do exist and are persistent throughout the entire thickness of the crystal, we assume that they are at least locally stable and that an equilibrium exists between the surface energy of the facets that bound the void and the elastic strain associated with the dislocation. The validity of this explanation, originally proposed by Frank [6], has been experimentally verified by the authors of the current paper [10]. Briefly, if the surface energy of the pipe is balanced against the strain energy associated with the defect, one finds that the pipe radius (r_0) should be proportional to the square of the Burgers vector (b); the relevant physical parameters that determine the proportionality are the surface energy (γ) and the shear modulus (G):

$$\frac{b^2}{r_0} = \frac{8\pi^2\gamma}{G}. \tag{1}$$

Assuming that the shear modulus of SiC is 200 GPa [11] and the surface energy is 4 J/m^2 [12], the b^2/r_0 ratio should be equal to approximately 16 Å, in reasonable agreement with observed values [10]. With a basis for their stability established, the most interesting question about this defect is, how does a super-dislocation with such a large Burgers vector form? As limiting cases, we can identify two possible origins for the super-dislocations: either they were created during the original nucleation of the homoepitaxial layer on the seed crystal or they formed from the coalescence of smaller dislocations. Each of these possibilities is considered below.

First, it is known that the density of micropipes in PVT grown 6H-SiC crystals is 10^2–10^3/cm^2 and that this figure is independent of the seed crystal defect structure. For example, even though Lely platelets are virtually dislocation and micropipe free, PVT crystals deposited on such seeds still have a high micropipe density. Thus, we conclude that while some of the defects might be inherited from the substrate, most of them must be created during the homoepitaxial growth process. Furthermore, small misfits at the interfaces between slightly misoriented, impinging nuclei during the initial stages of growth are expected to generate arrays of unit dislocations, not the energetically costly super-

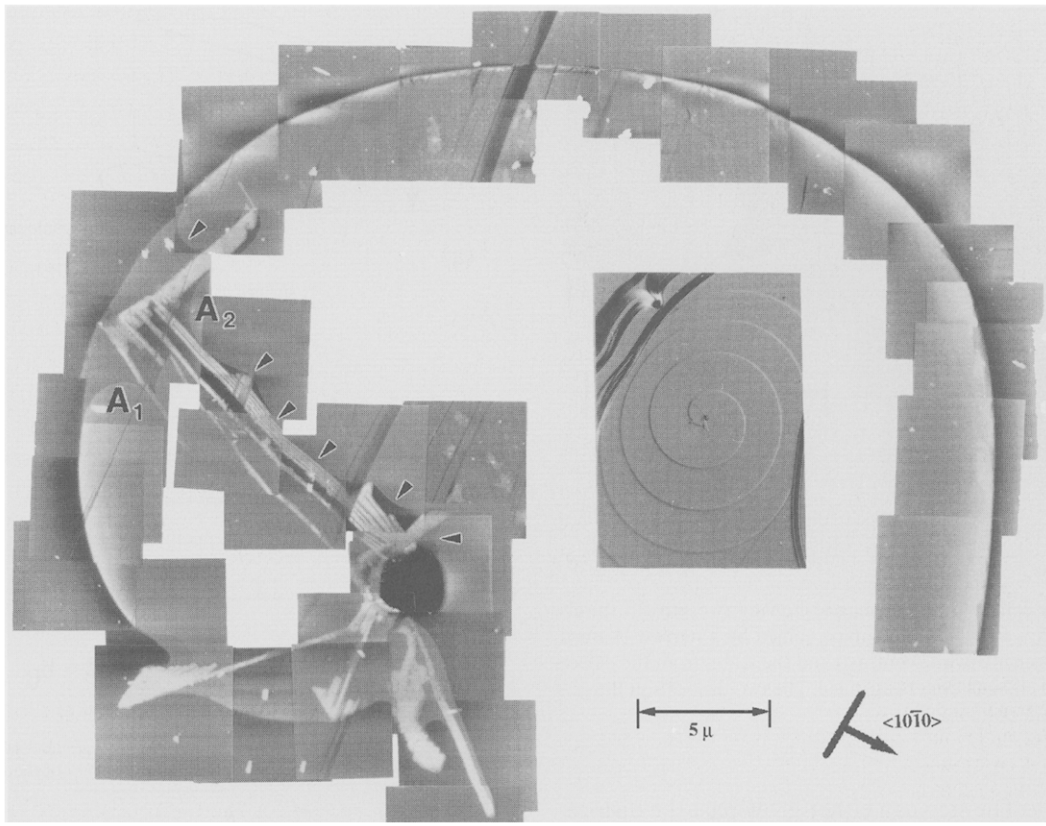

Fig. 6. A collage of AFM images showing a super-dislocation/micropipe complex and heterogeneous material (white contrast) that interrupts the flow of moving steps. The heterogeneity prevents steps moving in opposite directions (labeled A_1 and A_2) from filling in a channel. The height of the main step (the Burgers vector of the super-dislocation) is $12b_0$. The inset is a Nomarski contrast optical micrograph of the same feature and is included to show the extended step structure of this defect.

dislocations that are observed to coincide with the micropipes.

The second limiting case is that they form by the coalescence of unit dislocations. This is counter-intuitive since screw dislocations with the same sign repel each other elastically and super-dislocations always have a greater energy than the sum of their component unit dislocations. Nevertheless, since they are at least locally stabilized through their interaction with the empty pipe, it is reasonable to consider the possibility that coalescence occurs under the influence of a driving force that is stronger than the mutual repulsions. One such force could be the motion of the large steps that are observed on the growth surface. While many crystals grow by the advancement of monolayer steps, the steps on the SiC surface are much larger. Most of those associated with the spirals and measured by AFM are hundreds of angstroms high and others, such as those shown in Fig. 2, are even larger. Many of the steps visible in the optical micrographs are larger than the vertical depth of field of the AFM (0.7 μm). To see how the motion of large steps can lead to dislocation coalescence, we need to consider what happens when a large step tries to grow over a position where a unit screw dislocation intersects the surface.

Fig. 8a and Fig. 8b shows a large step, of height h, advancing across a surface towards the point where a dislocation line intersects the surface,

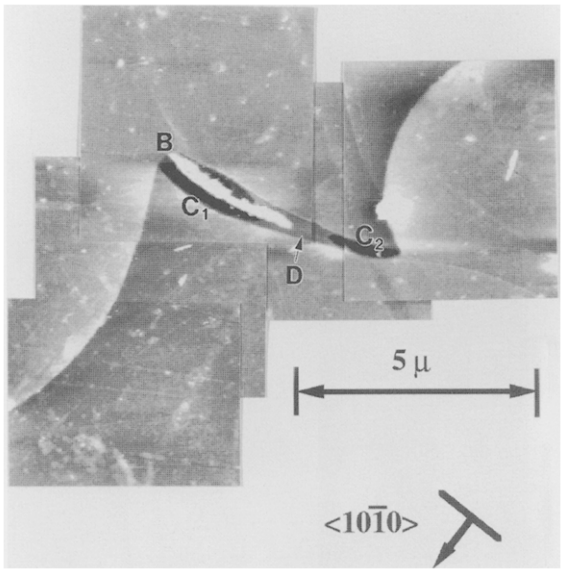

Fig. 7. A collage of AFM images showing two growth spirals, each with a small oval micropipe, joined by a narrow channel. A heterogeneity (white contrast) and the strain from the defects keeps the channel from being filled. The two dislocation Burgers vectors are both $5b_0$.

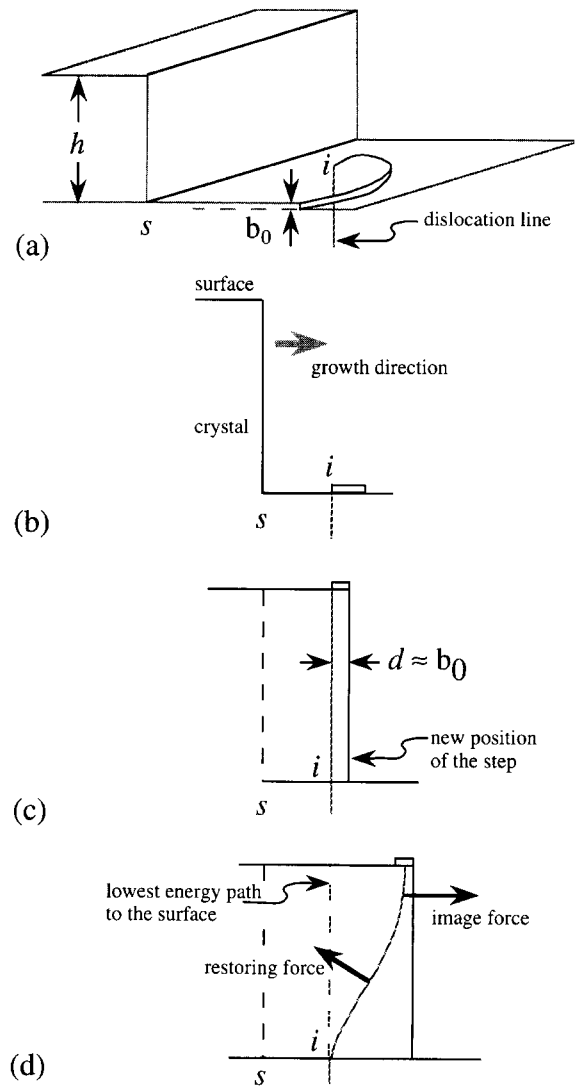

Fig. 8. Schematic illustration of a large step growing over the position where the line of a screw dislocation intersects the surface. (a) An oblique view, (b) a side projection, (c) new line is formed as the step grows just past the surface/dislocation intersection, (d) the line remains near the edge of the advancing step.

labeled *i*. The step can either grow past the dislocation line, creating new strained crystal above point *i* at a cost of approximately $1/2\mathrm{h}Gb_0^2$, (where G is the shear modulus) or it can bend the dislocation line, increasing its length by Δl at a cost of approximately $Gb_0^2\Delta l$, so that the end of the dislocation line remains fixed to the step edge. Obviously, as long as Δl is small in comparison to $h/2$, the dislocation line will extend through the newly grown crystal along a bent path, following the advancing step to lower the total elastic strain. Using this idea, we can estimate how high a step has to be to make the dislocation line move with it. The argument we use for this approximation relies on the assumption that the line of the dislocation in the already grown crystal is more or less fixed. In other words, the direction of the dislocation line will change only when new crystal is grown and the path introduced during growth will persist in the bulk. This assumption can be justified by considering the fact that if the line is bent away from the *c*-axis in any direction other than the glide plane, jogs of edge character are created. Bending the line out of the glide plane is, therefore, a nonconservative process and requires the long range diffusion of point defects. We assume that this occurs relatively easily at the growth surface but only very slowly in the bulk and, therefore, bending introduced during growth is kinetically stable in the bulk.

If a step of height h (where $h \gg b_0$) grows a very small distance (d) past the line of the dislocation (see Fig. 8c), then the new portion of the dislocation line feels an attractive image force, $-F_i = Gb^2/4\pi d$, which compels the dislocation line to remain very near or even attached to the step edge. To keep the dislocation line attached to the step, it must eventually be bent to a minimum radius of $h/2$ (see Fig. 8d). Thus, there will also be a repulsive restoring force that tends to minimize the length of the line by pulling it away from the step so that it forms a straight line parallel to the c axis. This force will maximize at $F_r = \alpha Gb^2/2h$, where α is a constant near unity, when the radius of curvature reaches its minimum value. Taking d to be a small number (i.e., we assume that very little new strained crystal is formed), equal to b_0, we see that as long as h is on the order of $8\pi b_0$ (approximately 400 Å) the step can "push" the dislocation line in a direction parallel to the step motion. When the minimum radius of curvature is reached, the step can grow only by breaking away from the dislocation line or by creating new edge segments parallel to the step growth direction. Even if the first case is true (as illustrated in Fig. 8) the dislocation line can be moved significant distances by the consecutive action of many steps. Finally, it is important to note that this same line of reasoning explains why the small monolayer steps found on most growth surfaces do not influence the directions of dislocation lines; smaller steps would require so much curvature that the restoring force exceeds the attractive image force and it takes less energy to grow over the dislocation line than to bend it.

The discussion above explains how a moving step can push a dislocation line. For dislocation lines to coalesce and form super-dislocations, it is necessary to push them to the same point. This can occur as a circular step decreases its length by contracting towards its center, a process shown schematically in Fig. 9. Based on our observations of the 6H-SiC(0 0 0 1) surface, we conclude that this situation occurs when moving steps encroach on the areas of the surface that are covered with the heterogeneous phase. For example, consider the steps labeled A1 and A2 that are growing towards one another around the heterogeneity in Fig. 6. When the two meet, the heterogeneity will be surrounded and then the step will continue to shrink towards the center. Eventually, if enough steps reach this point, the surrounding step will become higher than the heterogeneity and overgrow it to form an inclusion. However, if the surrounding step drags dislocation lines toward the center, the elastic stress from the defects will prevent the void from being filled and a super-dislocation/micropipe complex will be formed. This could explain how the defect in Fig. 6 was formed.

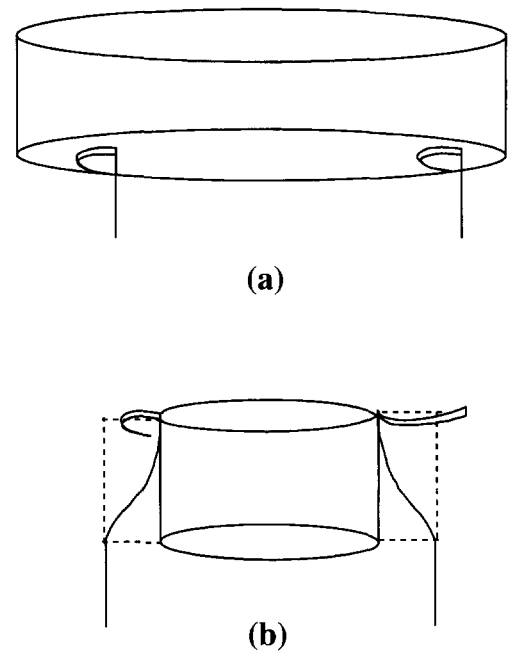

Fig. 9. (a) A circular step forms a well in the crystal. Two screw dislocations intersect the surface at the bottom of the well. (b) As the crystal grows, the length of the step and the well radius shrinks until it reaches the points were the dislocations intersect the surface. As the step continues to shrink, the dislocations remain near the step.

The observation that best illustrates this process is shown in Fig. 7. The heterogeneity labeled B is completely surrounded by a step that forms an oval void; the presence of the heterogeneity prevents crystal from growing in this void. As large steps from other sources sweep over this point, more circular steps surrounding the heterogeneity will be left behind and as they shrink, the two dislocations at either end of the channel will be drawn

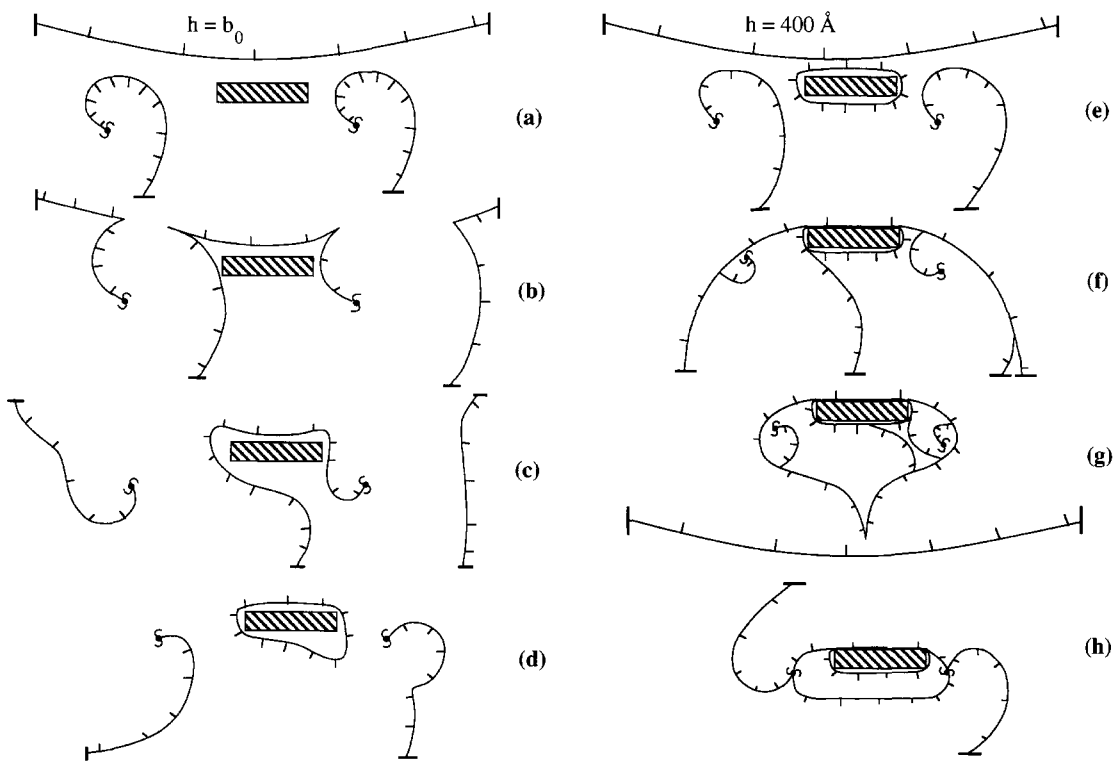

Fig. 10. Projected views of intermediate steps in the proposed super-dislocation/micropipe complex formation mechanism. For a detailed explanation, see the text.

progressively towards one another until a local equilibrium is established between elastic strain associated with the defects and the surfaces of the void. At this point, the heterogeneity is no longer needed to keep the void from being filled in, crystal growth in the space between the dislocations will be retarded by the elastic strain.

The details of our proposed mechanism for super-dislocation/micropipe complex formation during vapor phase growth are illustrated in Fig. 10. Fig. 10 shows a plan view of the surface and each line on the diagram represents a step that is hatched on the "uphill" side. The steps that are terminated by short perpendicular segments at the edge of the figure are assumed to continue outside the boundaries of the drawing. Those that end within the drawing represent step origins at the points where screw dislocations intersect the surface. The rectangular cross-hatched object is a surface heterogeneity. For the proposed mechanism to work, the surface heterogeneity must be immobile so that it can not be pushed across the surface in front of an advancing step. A trapping mechanism that can immobilize the heterogeneity is depicted in Fig. 10a–Fig. 10d. If a step of height b_0 advances from a distant source, it will annihilate portions of each of the spiral steps (see Fig. 10b) and leave a step that forms and incomplete loop around the heterogeneity (see Fig. 10c). As growth continues, two parts of the same step meet to form a closed loop around the heterogeneity (see Fig. 10d) and, at this stage, it is partially buried and assumed to be immobile.

After immobilization, a large step ($h > 400$ Å) may sweep past and form a closed loop around the particle and the dislocations (see Fig. 10e–Fig. 10g). As the loop shrinks, the dislocations will be trapped on the walls and bent, as described

above (see Fig. 10g). Other passing steps will draw the dislocations closer and closer to the central empty region. Eventually, the loop radius will stabilize at a point where the surface energy of the wall is balanced by the strain energy from the dislocations and the locally stable super-dislocation/micropipe complex is formed.

There are three elements that are necessary for this mechanism to be operative. First, isolated, unit screw dislocations are needed to feed the process. A pair of these defects (labeled A_3 and A_4) are apparent in Fig. 5 and synchrotron X-ray topography indicates that the density of these defects is on the order of $10^4/cm^2$ [9]. Considering this density and assuming that each defect has 6 near neighbors, the formation of a super-dislocation with $b = 7b_0$ by coalescence requires each neighboring defect to migrates less than 100 μm. Since the crystal grows vertically by hundreds of times this length scale as steps continuously sweep across the surface, each step would have to move a dislocation line laterally by only a small fraction of its height to drive the proposed coalescence reaction. Second, immobilized surface heterogeneities are required to create the shrinking step that surrounds the dislocations. Many examples of this heterogeneous material have been observed and two particularly instructive cases are presented in Figs. 6 and 7. Finally, large steps, hundreds of angstroms in height are required. These are observed on all parts of the surface by both optical microscopy and AFM.

The lateral forces from moving steps might also drive dislocation annihilation reactions. We assume that the initial population of screw dislocation orientations is more random than the final clustered distribution. The final distribution could be formed if, during growth, equal numbers of dislocations with opposite orientations are annihilated until only those of the same orientation remain.

Based on the AFM data presented here, it is impossible to unambiguously identify the heterogeneous material observed on the SiC growth surface. Candidates include elemental Si or C, deposited during unanticipated deviations from stoichiometry, or carbide and silicide compounds formed from transition metal impurities in the source material. Considering the amount of heterogeneous material that is observed, it seems more likely that it is C or Si than an impurity. Furthermore, if it was actually molten during growth, as it appears, Si is the more likely of the two candidates. The observation of cubic faceting is consistent with the tentative assignment that the material is Si.

5. Conclusion

In the PVT process, 6H-SiC grows by a spiral mechanism. While some of the steps are as small as 15 Å, super-dislocations and step bunching leads to others that are many hundreds of angstroms in height. The strain associated with the super-dislocations is locally stabilized by the formation of a micropipe. Near the surface/micropipe intersection, we have observed a heterogeneous phase that influences the motion of growth steps. We have proposed a mechanism in which the large steps interact with unit screw dislocations and the heterogeneous phase to form the super-dislocation/micropipe complexes.

Acknowledgements

The authors acknowledge helpful discussions with Professor W. Mullins and the assistance of N.T. Nuhfer in recording optical micrographs. This work was supported by the Office of Navel Research under Grant N00014-96-1-0944. J.G. acknowledges support from an NSF REU supplement to YIA Grant No. DMR-9458005.

References

[1] B.J. Baliga, IEEE Electron. Device Lett. 10 (1989) 455.
[2] D.L. Barrett, J.P. McHugh, H.M. Hobgood, R.H. Hopkins, P.G. McMullin, R.C. Clarke, W.J. Choyke, J. Crystal Growth 128 (1993) 358.
[3] R.C. Glass, L.O. Kjellberg, V.F. Tsvetskov, J.E. Sundgren, E. Janzen, J. Crystal Growth 132 (1993) 504.
[4] H.M. Hobgood, D.L. Barrett, J.P. McHugh, R.C. Clarke, S. Sriram, A.A. Burk, J. Greggi, C.D. Brandt, R.H. Hopkins, W.J. Choyke, J. Crystal Growth 137 (1994) 181.
[5] J.A. Powell, P.G. Neudeck, D.J. Larkin, J.W. Yang, P. Pirouz, Inst. Phys. Conf. Ser. 137 (1994) 161.
[6] F.C. Frank, Acta Crystallogr. 4 (1951) 497.

[7] A.R. Verma, Crystal Growth and Dislocations, Butterworths, London, 1953.
[8] H. Tanaka, Y. Uemura, Y. Inomata, J. Crystal Growth 53 (1981) 630.
[9] M. Dudley, S. Wang, W. Huang, C.H. Carter Jr., V.F. Tsvetkov, C. Fazi, J. Phys. 28 (1995) A63.
[10] J. Giocondi, G.S. Rohrer, M. Skowronski, V. Balakrishna, G. Augustine, H.M. Hobgood, R.H. Hopkins, in: D.K. Gaskill, C.D. Brandt, R.J. Nemanich (Eds.), III-Nitride, SiC, and Diamond Materials for Electronic Devices, vol. 423, Mater. Res. Soc. Proc., Pittsburgh, PA, 1996, p. 539.
[11] W.R.L. Lambrect, B. Segall, M. Methfessel, M.V. Schilfgaarde, Phys. Rev. B 44 (1991) 3685.
[12] B. Wenzien, P. Käckell, F. Bechftebt, Surf. Sci. 307 (9) (1994) 989.